JMEPEG (2006) 15:540-548
DOI: 10.1361/105994906X136052

1059-9495/$19.00

Effect of Cold Work on the Tensile and Fatigue Performance of Aluminum Alloy 5754

Zheng Jin and P.K. Mallick

(Submitted July 26, 2005)

This article considers the effects of cold work on the tensile and fatigue properties of a non-heat-treatable aluminum alloy, namely, AA5754. Cold work up to 50% was introduced by cold rolling. The critical tensile strain for serration initiation was observed to increase with increasing cold work. The fatigue performance was also improved with increasing cold work. Annealing at 200 °C for 1 h reduced both the critical strain as well as the fatigue performance. Finally, in experiments with drilled holes and punched holes, it was observed that punching improved the fatigue performance compared with drilling, which was attributed to cold work induced at the hole boundary by the punching operation.

Keywords aluminum alloy 5754, annealing, cold work, drilled hole, fatigue, punched hole

1. Introduction

The effect of cold work on the fatigue properties of steel has been the subject of several published studies in the past, but not much information is available regarding aluminum alloys. The cold work in the experiments conducted on steel was induced either by cold rolling or by tensile prestraining. Yu et al. (Ref 1) conducted strain-controlled fatigue tests on a high-strength, low-alloy (HSLA) steel that was cold-rolled to 30 and 61% thickness reductions. Cold rolling significantly improved the fatigue strength of the material. At 30% cold work, the fatigue strength improved by 20% in the length direction and by 37.5% in the transverse direction over that of the hot-rolled condition. At 61% cold work, the fatigue strength improvement was even greater: 28.5% in the rolling direction; and 52% in the transverse direction. Yu et al. (Ref 1) also observed that the notch sensitivity of the cold-rolled specimens was higher, although the notch sensitivity did not change much with the increase in cold work. Sherman (Ref 2), on the other hand, did not observe much effect of cold rolling on the fatigue performance of a different HSLA steel. In that case, the material was cold-rolled to a 20% thickness reduction. The strain-life curve of the cold-worked specimens was virtually the same as that of the hot-rolled HSLA steel except for long lives for which the cold-rolled material was slightly superior. Raman and Padmanabhan (Ref 3) conducted strain-controlled fatigue tests on an austenitic stainless steel that was cold-worked to 10, 20, and 30% reduction in area by rotary swaging. They observed that above a strain amplitude of 0.5% the fatigue life decreased with increasing cold work, but the converse was true below this strain amplitude.

In the published research on the effect of prestrain on fatigue, the fatigue specimens were machined from a flat sheet or strip after prestraining it in tension. The prestraining level was usually in the range of 5 to 20% strain. Sherman (Ref 2) observed that tensile prestrain resulted in a reduction in the fatigue life of HSLA steel at all strain amplitude levels. In a separate study, Sherman and Davies (Ref 4) observed an improvement of the strain-life curve of a dual-phase steel when a tensile prestrain up to 8% was imposed, which was in contrast to the study on HSLA steel. Nagase and Suzuki (Ref 5) conducted stress-controlled bending fatigue tests on round specimens of a 1025 steel, with and without tensile prestrain. They observed that the fatigue life decreased significantly at 3% prestrain, while a 7% prestrain did not cause any change relative to the annealed condition. Radhakrishnan and Baburamani (Ref 6) conducted reverse-bending fatigue tests on a 0.26% carbon steel and a stainless steel. The tensile prestrain was 6, 9, and 13% for the carbon steel, and 10, 20, and 30% for the stainless steel. In both cases, fatigue strength improved with increasing prestrain, and the increase in the endurance limit was found to be directly proportional to the degree of prestrain. In the crack propagation study with the same materials (Ref 6), they also observed that increasing the prestrain level increased the crack nucleation period, but the crack propagation rate was reduced.

Sonsino (Ref 7) reported the effect of 1 and 5% tensile prestrain on the crack initiation life of a structural steel and an

Zheng Jin and **P.K. Mallick,** Center for Lightweighting Automotive Materials and Processing, University of Michigan-Dearborn, Dearborn, MI 48128. Contact e-mail: pkm@umich.edu.

Table 1 Chemical composition of aluminum alloys 5754-O (wt.%)

Alloy	%Si	%Fe	%Cu	%Mn	%Mg	%Cr	%Ni	%Sn	%Ti	%Pb	%Al
5754-O	0.07	0.07	<0.01	0.44	3.0	<0.01	<0.01	<0.01	<0.01	0.01	Base

Source: Ref 9

age-hardened Al-Cu-Mg alloy in both strain-controlled and load-controlled fatigue tests. The crack initiation life was defined as the number of fatigue cycles needed to develop a 1 mm deep crack. For both materials, crack initiation life decreased with increasing prestrain. At 5% prestrain, the crack initiation life decreased by approximately 30% in the strain-controlled tests and by 50% in the load-controlled tests.

Lanning et al. (Ref 8) examined the effect of a tensile prestrain of between 1 and 5% on the high cycle fatigue life of a Ti-6Al-4V titanium alloy. They used a step-loading method in which the stress in subsequent steps was incrementally increased (typically 5%) if the specimen did not fail in 10^6 cycles in the previous step. The cyclic stress ratio, R, was 0.1 and 0.5, respectively. They observed a small decrease in fatigue strength at 10^6 cycles with increasing tensile prestrain at $R = 0.1$ and no discernible effect at $R = 0.5$.

In this article, the effect of cold work on the static and fatigue performance of aluminum alloy 5754 was studied. This material is representative of the 5xxx series aluminum-magnesium alloys considered for automotive body structures. The cold work was introduced by subjecting the as-received O-tempered sheet of AA5754 to various levels of thickness reduction by cold rolling. In addition, the effect of cold work induced by rivet punching was also investigated.

2. Experimental

2.1 Material

Several 2 mm thick sheets of AA5754-O were obtained. The composition of the particular 5754-O alloy used is shown in Table 1. The following cold work and annealing conditions were considered in this work:

- As-received (assumed to be at 0% cold work level)
- As-received and annealed at 200 °C for 1 h
- As-received and annealed at 260 °C for 1 h
- Cold rolled to 5, 20, 30, 40, and 50% cold work level
- Cold rolled to 5, 20, 30, 40, and 50% cold work level and subsequently annealed at 200 °C for 1 h
- Cold rolled to 20 and 40% cold work level and subsequently annealed at 260 °C for 1 h

The as-received sheet was cold-rolled to the desired cold work level in a single pass in a laboratory-sized two-roll rolling mill with a 203 mm roll diameter. The amount of cold work was calculated from the thickness reduction. The annealing experiments were performed in a preheated air-circulating oven. After keeping the specimens in the oven for 1 h, they were allowed to cool down slowly outside the oven. For a normal paint-baking operation in the automotive industry, the maximum paint bake temperature is 200 °C and the baking cycle lasts 30 to 40 min (Ref 10). The annealing condition of 200 °C for 1 h used in this study is similar to the paint-baking condition. The other annealing condition, namely, 260 °C for 1 h, was selected to represent an extreme paint-baking condition.

2.2 Microstructure

To examine the microstructures, specimens were cold-mounted using an epoxy resin, and then sequentially ground using 240, 320, 400, 600, and 1200 grit silicon carbide grinding papers. They were then manually polished using a 3 μm diamond spray and followed by 1 μm alumina suspension. Finally, the specimens were subjected to electrolytic etching in Barker's solution consisting of 45 mL of purified fluoroboric acid (48 ~ 50%) in 200 mL of deionized water.

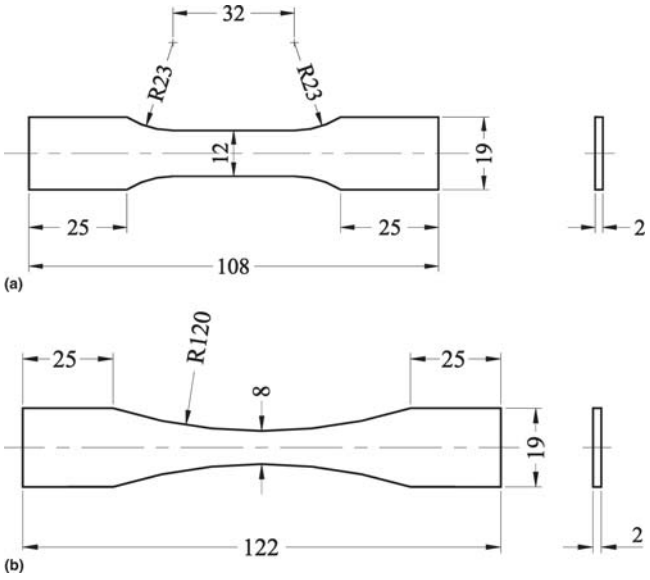

Fig. 1 Schematic of (a) tensile specimen and (b) fatigue specimen (dimensions are in millimeters)

2.3 Hardness Measurements

Rockwell superficial hardness was used for surface hardness measurements of the sheets. Each specimen surface was indented at three separate locations using the 15T scale and a 1/16 in. diameter steel ball as the indenter, and the average hardness was calculated from the three readings. In addition, Knoop microhardness was measured on polished cross sections of the AA5754 sheet using a 15 kg major load and a 3 kg minor load on a Clark (Instron Corp., Canton, MA) (model DMH-2) microhardness tester. For each specimen, five indentations were made randomly at different locations on the cross section. The reading of each indentation was taken at a 50 gram force load level. The loading time was 15 s.

2.4 Tension and Fatigue Tests

The tensile specimens, schematically shown in Fig. 1(a), were machined in the rolling direction. Monotonic tension tests were conducted on an MTS 810 (MTS Systems Corp., Eden Prairie, MN) servohydraulic testing machine. An extensometer (25 mm gage length) was mounted on the middle section of each specimen during the test. The crosshead speed was 1.27 mm/min, which was approximately equivalent to a strain rate of 8.5×10^{-4} s^{-1}. Two specimens were tested for each condition of cold rolling and for each condition of cold rolling followed by annealing. In addition to the cold-worked and annealed specimens, a few specimens were tested with a centrally drilled hole and a centrally punched hole. The hole diameter was 3 mm. The punched hole was created by driving a steel rivet through the specimen in a self-piercing riveting machine. A 5 mm long backup strip was used under the specimen, and even though this strip was connected to the specimen by the

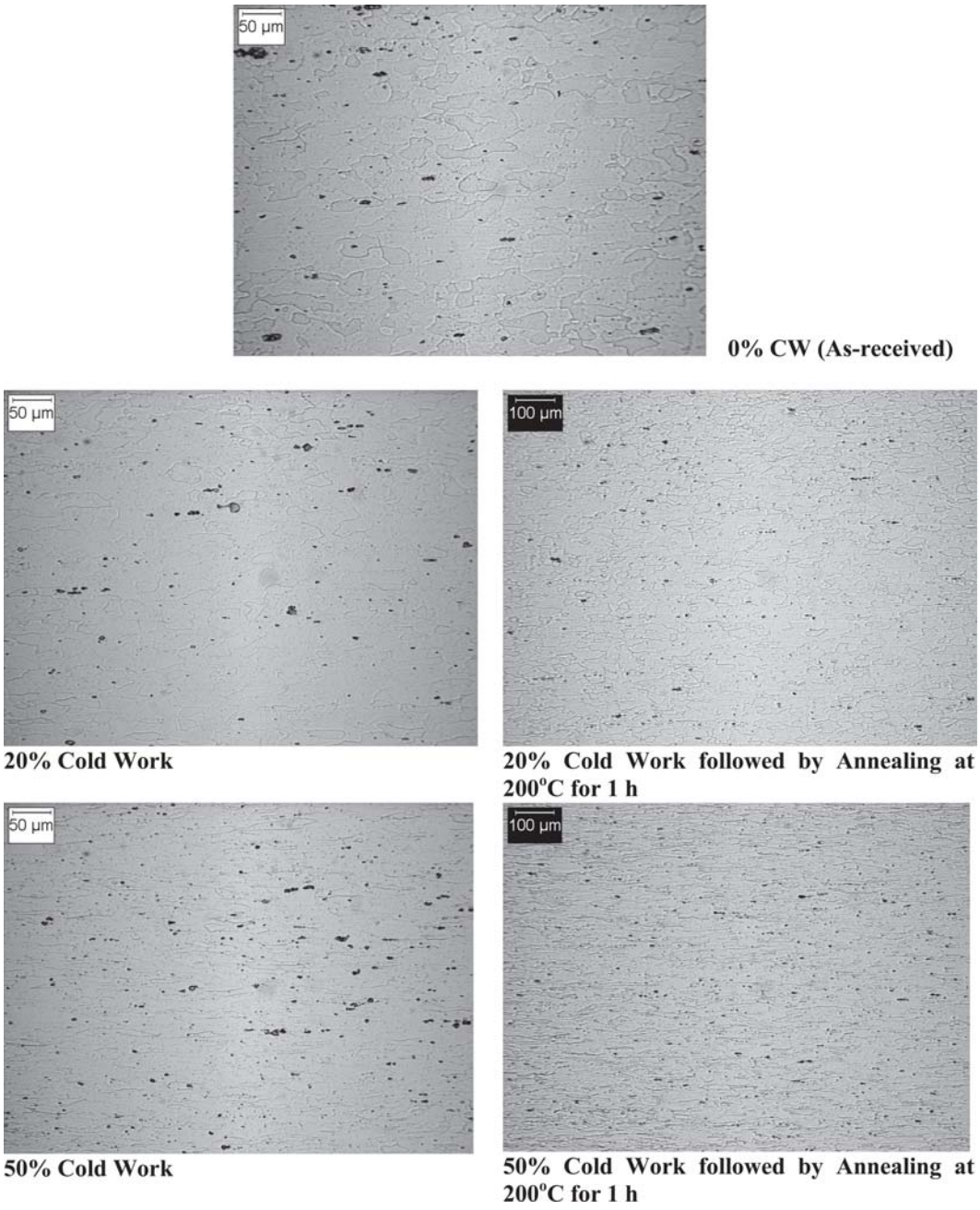

Fig. 2 Microstructures of AA5754 sheets

rivet, it did not share any load during the tension and fatigue tests. Replicate tests were conducted for each type of specimen.

Fatigue tests were performed on the MTS machine using a tension-tension load control mode at 15 Hz. Because straight-sided fatigue specimens without the central hole did not fail in the gage area, fatigue tests were conducted with hourglass-shaped specimens with a continuous radius of 120 mm (Fig. 1b). Fatigue tests with the central hole were conducted with straight-sided, dog bone-shaped specimens of the type shown in Fig. 1(a). The minimum-to-maximum stress ratio (R) in all fatigue tests was 0.1. For each condition, four to five load levels were selected corresponding to 90, 80, 70, 60, and 50% of the average peak stress observed in the tension tests. Most of the specimens were tested until failure by separation.

3. Results

3.1 Microstructures

The microstructures of the cold-rolled 5754 sheets at 0% (as-received), 20 and 50% are shown in Fig. 2. In the as-received sheets, the grains were not completely equiaxed, even though the material in the as-received sheets was in O-temper. According to Court et al. (Ref 11), this may be due to the addition of Mn, which tends to produce slightly elongated grains. The microstructure also showed numerous randomly dispersed particles, which are probably mostly Al_6Mn particles, although some of them may also be compounds with Fe or Si (Ref 12). Increasing the amount of cold work produced even more elongated grains in the roll-

ing direction; however, only at 40 and 50% cold work levels were the grains highly elongated in the rolling direction. The dispersed particles were also elongated in these specimens. Annealing at 200 or 260 °C for 1 h did not significantly change the grain structure from the nonannealed conditions.

3.2 Hardness and Tensile Properties

The average hardness and tensile properties of the cold-rolled specimens as well as the annealed specimens are listed in Table 2. Both superficial Rockwell hardness and Knoop hardness increased with increasing cold work. Annealing decreased the hardness at each cold work level. The higher annealing temperature caused a slightly larger decrease in hardness. The decrease in hardness with annealing indicates that there was some recovery during the annealing stage, even though neither the annealing temperature nor the annealing time was very high.

Typical engineering stress-strain curves of the as-received and cold-worked AA5754 specimens are shown Fig. 3. In each curve, there was clear evidence of serrated flow, which is commonly observed in many 5000 series aluminum alloys. In addition, the as-received specimen showed a small yield plateau, which did not appear in stress-strain diagrams of the cold-worked specimens. Following the classification scheme described by Robinson and Shaw (Ref 13), the serrated flow was classified as type C in the as-received specimen, a combination of types B and C in 5 and 20% cold-worked specimens, and type C in 30, 40, and 50% cold-worked specimens. All of the specimens failed by local necking in the gage area. The local necking was formed at an angle with the loading axis. For the as-received sheet, this angle was 75°, and it decreased with increasing cold work.

Figure 4 shows the tensile stress-strain curves of the annealed specimens. As with the cold-worked specimens, the annealed specimens also exhibited serrated flow. For the as-received specimens, annealing at either 200 or 260 °C did not change the nature of the serrated flow, which was of type C for all three conditions. For the 20% cold-worked specimens, the type of serrated flow changed from a combination of B and C to only C when the annealing temperature was 260 °C. For the

Table 2 Hardness and tensile data of as-received, cold-rolled, and annealed AA5754 sheet

Cold work level	Superficial Rockwell hardness	Knoop hardness	0.2% yield strength, MPa	Tensile strength, MPa	YS to TS ratio	Uniform elongation, %	Critical strain, %
Cold-worked, but not annealed							
0%	66.8	70.6	110	242	0.454	20.8	0.30
5%	71	76.9	160	249	0.642	17.3	0.85
20%	75.4	80.9	247	288	0.858	4.8	1.27
30%	77.5	85.9	268	305	0.879	4.7	1.48
40%	79.5	90.2	321	359	0.894	4.6	1.48
50%	81.4	91.9	305	335	0.910	4.3	1.33
Annealed at 200 °C for 1 h after cold work							
0%	64.8	65.9	96	237	0.405	19.0	0.18
5%	66.4	69.1	128	247	0.518	17.6	0.61
20%	73.9	76.2	181	268	0.675	12.0	1.12
30%	75	80.6	201	280	0.718	10.9	1.35
40%	76	87.3	220	292	0.753	9.7	1.35
50%	76.8	89.9	228	291	0.783	8.9	1.30
Annealed at 260 °C for 1 h after cold work							
0%	61.6	61.7	100	246	0.406	20.5	0.17
20%	71.8	73.6	160	260	0.615	12.8	0.26
40%	73.5	83.9	176	255	0.690	10.1	0.95

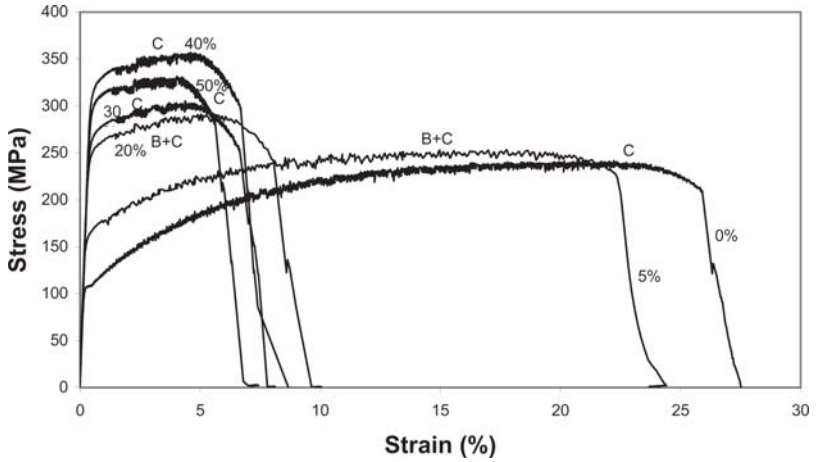

Fig. 3 Tensile stress-strain curves of as-received and cold-worked AA5754 sheets. The percentage of cold work and serrated flow type are indicated in the figure.

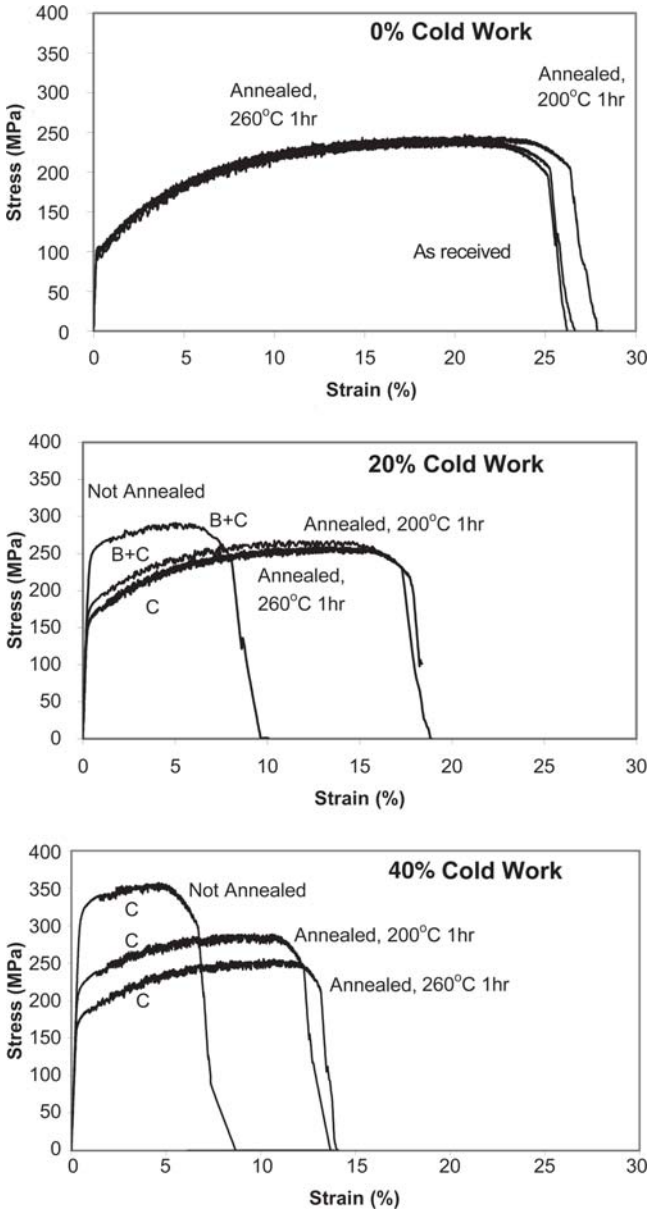

Fig. 4 Effect of annealing (at 200 and 260 °C for 1 h) on the tensile stress-strain curves of as-received and cold-worked specimens

40% cold-worked specimens, the serrated flow again was of type C in the cold-worked and annealed conditions.

For the as-received sheet, the yield strength (YS) and ultimate tensile strength (UTS) were 110 and 242 MPa, respectively. The uniform plastic elongation was 20.8% and the total elongation was 25.9%. Annealing at 200 and 260 °C for 1 h did not cause any appreciable changes in the YS, UTS, and elongation of the as-received specimens (0% cold work). Both YS and UTS increased with increasing cold work up to 40% cold work and then decreased slightly at 50% cold work. The uniform elongation, on the other hand, decreased sharply after 5% cold work and remained nearly constant at 20 to 50% cold work values. The YS and UTS of the annealed specimens were lower, and both decreased with increasing annealing temperature. The ratio of YS to UTS increased with increasing cold work, but for each cold work level it decreased with annealing. The uniform elongation of the annealed specimens was considerably higher than that of the 20 to 50% cold-worked specimens. It also decreased steadily with increasing cold work. However, there was only a small difference in the uniform elongations of the 200 and 260 °C annealed specimens.

A significant feature of serrated deformation curves is the occurrence of an incubation period before the onset of serrated flow. The critical strain ε_c signifies the end of this incubation period. A higher critical strain is desirable for more homogeneous plastic deformation and greater formability. In the AA5754 alloy, the critical strain increased with increasing cold work (Table 2). The effect of annealing, on the other hand, was to reduce the critical strain. Annealing at 260 °C caused a higher reduction in critical strain than annealing at 200 °C.

Figure 5(a) to (c) show the fracture surfaces of the tension specimens. On the fracture surface of the as-received specimen, a large number of dimples of different sizes and shapes was visible, indicating ductile failure. Particles of various sizes and shapes were clearly visible inside many of the dimples. In aluminum alloys, dimples are initiated as microvoids in the second-phase particles (Ref 14). The size and shape variations of the dimples are usually attributed to the size and shape variation of the second-phase particles. In the case of the AA5754 alloys, these particles are the Al_6Mn or other intermetallic compounds observed in the microstructure shown in Fig. 2. In the midthickness of the as-received tension specimens, several large craters were observed (Fig. 6a). Dimples were also found on the walls of these craters. A high-magnification view of the inside of some of these craters showed a layered structure (Fig. 6b). This may be due to void growth taking place in steps.

Tensile fracture surfaces of the 5 to 50% cold-worked specimens also contained numerous dimples; however, it appears that the number of dimples decreased with increasing cold work. For the 20 to 50% cold-worked specimens, the dimples appeared to be slightly elongated in the direction of the axial tensile stress. Second-phase particles were visible deep inside many of these dimples (Fig. 7). The void formation started around these particles.

3.3 Fatigue Properties

The diagrams of stress versus number of cycles (*S-N*) of the as-received, cold-worked, and annealed specimens are plotted in Fig. 8 with the maximum fatigue stress along the vertical axis, and the log numbers of cycles to failure along the horizontal axis. For the majority of the fatigue specimens, the maximum fatigue stress level was either 70 or 80% of the UTS of the material. Except for the as-received and 5% cold-worked specimens, these maximum stress levels were below the YS of the cold-worked material. The maximum stress levels for the as-received and cold-worked specimens were significantly above the YS.

The *S-N* diagrams indicate that the cold-worked specimens had a better fatigue performance than the annealed specimens. This was particularly true for the 20 and 30% cold-worked specimens. When the fatigue data of all the cold-worked specimens were compared (Fig. 9), the fatigue performance of the AA5754 alloy was found to improve with increasing cold work up to 40% cold work. The specimens with 50% cold work did not show any improvement over specimens with 40% cold work. A similar trend was observed with specimens annealed at 200 °C for 1 h (Fig. 10).

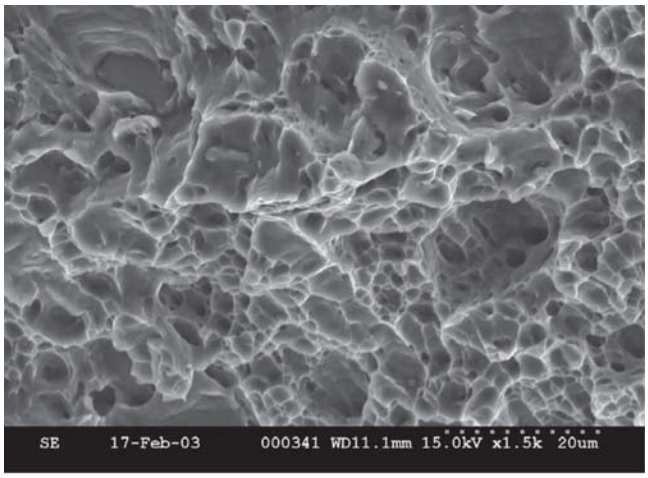

(a)

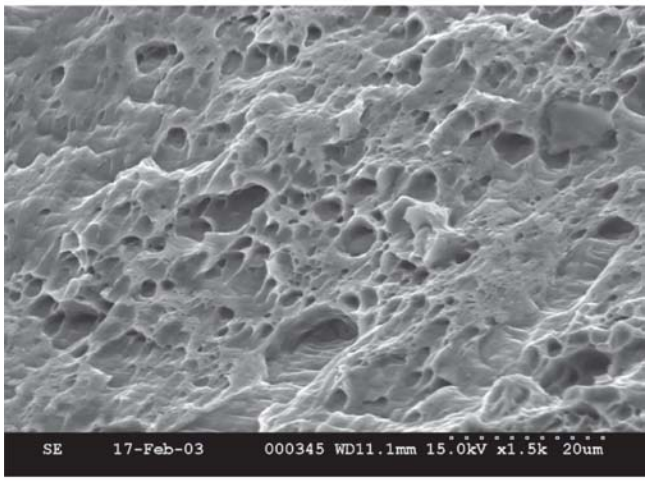

(b)

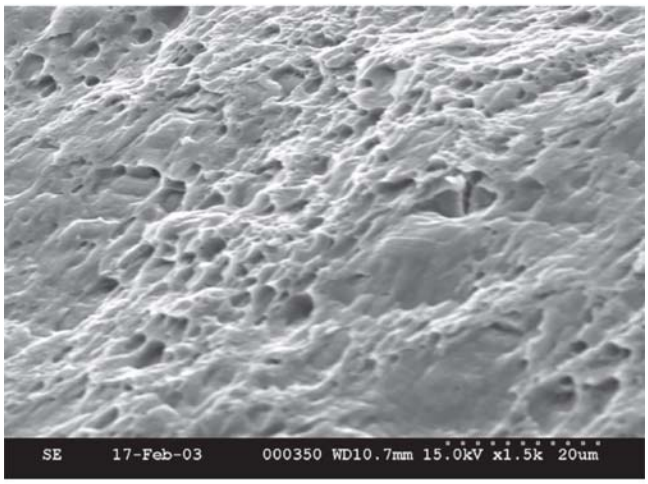

(c)

Fig. 5 SEM photographs showing the fracture surfaces of the tensile specimens: (a) 0% cold work; (b) 20% cold work; (c) 50% cold work

Figure 11 shows the scanning electron microscopy (SEM) photograph of the fracture surface of one of the as-received fatigue specimens that had been subjected to a maximum stress level equal to 70% of the static strength. In this case, the fatigue

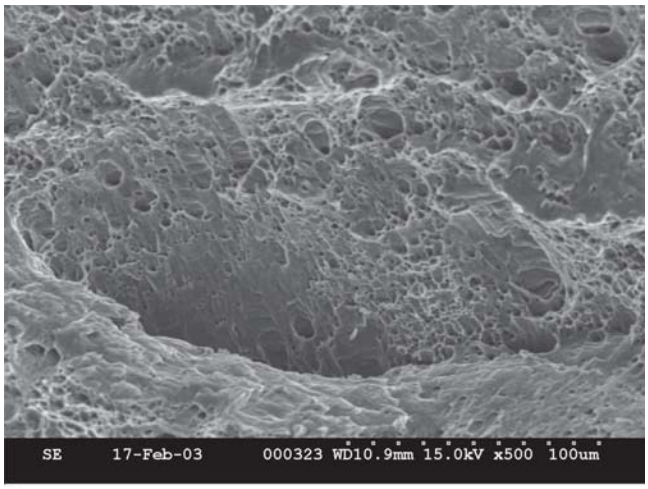

(a)

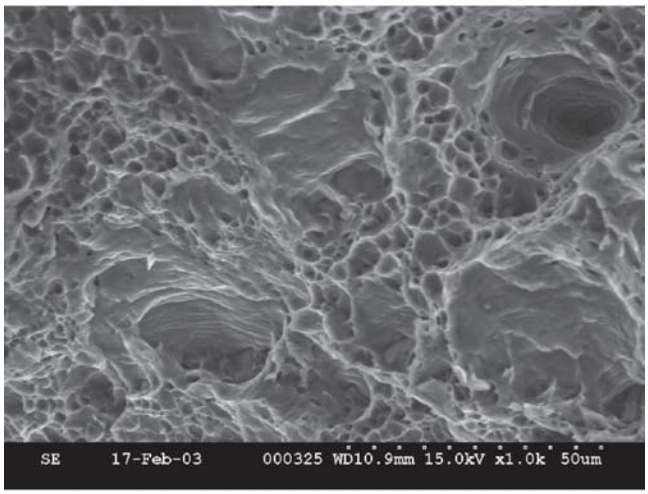

(b)

Fig. 6 SEM photograph showing (a) the close-up view of a large crater and (b) a layered structure inside the craters on the tensile fracture surface of an as-received specimen

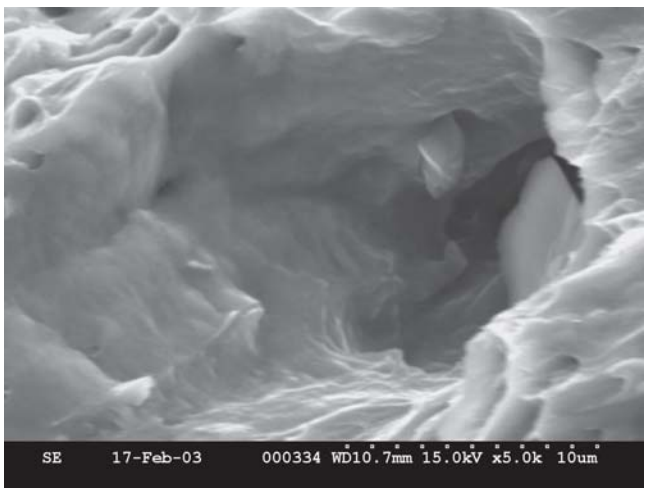

Fig. 7 SEM photograph showing a second-phase particle inside one of the craters

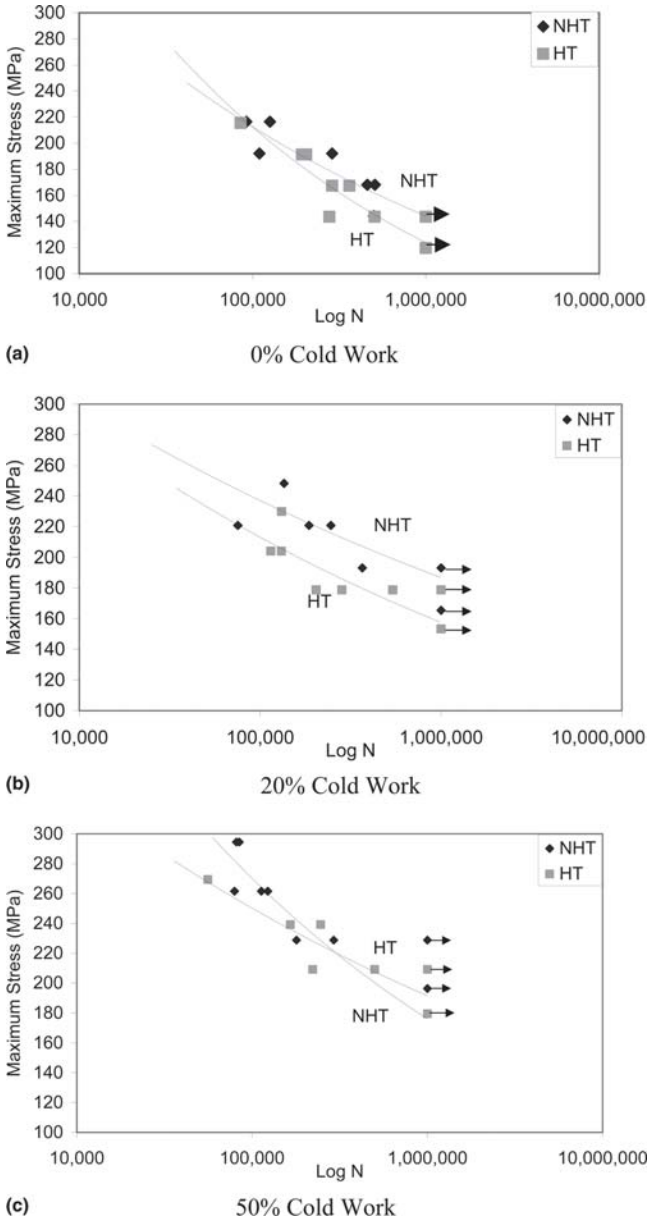

Fig. 8 *S-N* diagrams of cold-rolled 5754 sheets at (a) 0% cold work (as-received), (b) 20% cold work, and (c) 50% cold work. NHT, not heat-treated; HT, heat-treated (annealed at 200 °C for 1 h)

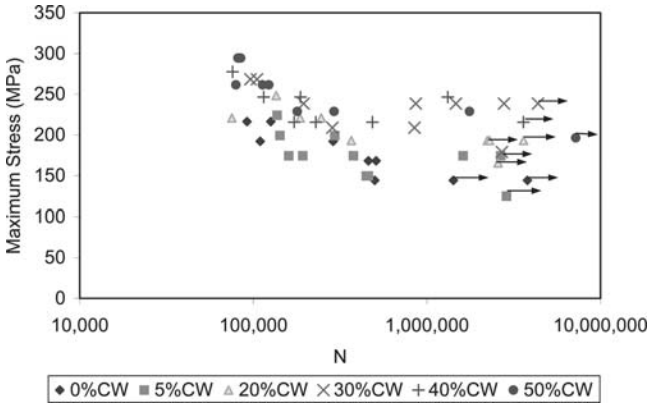

Fig. 9 *S-N* diagrams of as-received and cold-worked specimens (not annealed)

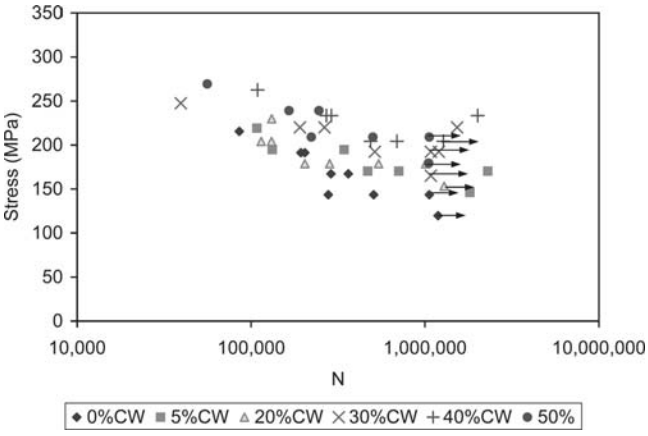

Fig. 10 *S-N* diagrams of as-received and cold-worked specimens after annealing at 200 °C for 1 h

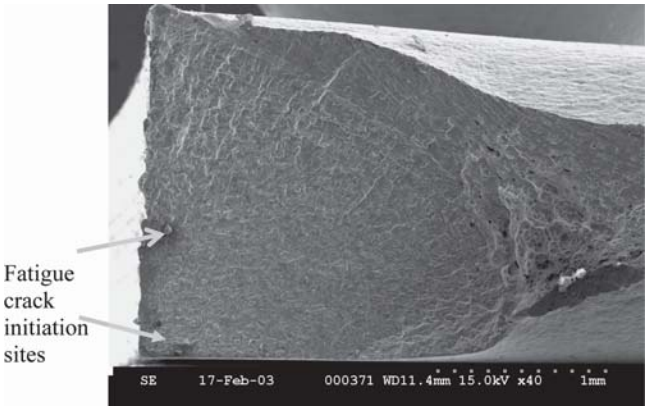

Fig. 11 SEM photograph showing the fatigue crack initiation sites on the fracture surface of an as-received specimen

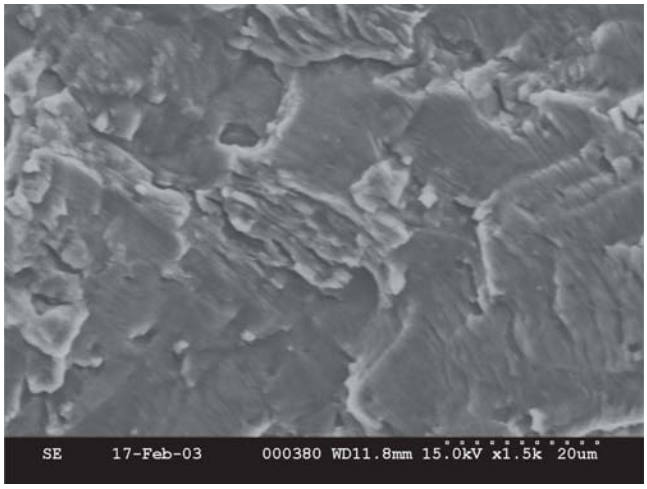

Fig. 12 SEM photograph showing striation marks on the fatigue fracture surface

crack initiated at the relatively large second-phase particles located near one of the edges of the specimen. Ahead of the slow fatigue crack growth area, there was a considerable amount of plastic deformation, which produced thinning of the specimen as well as of the appearance of the dimples in the

final fracture region. Striation marks were visible on some of the facets on the fracture surface (Fig. 12). Similar fracture surface appearances were also observed for the 5, 20, and 30% cold-worked specimens; however, with an increasing amount of cold work, there was less plastic deformation. Inside the dimples of the fatigue specimens, second-phase particles were visible, indicating that dimples were created by void formation around the particles. The location of the fatigue failure initiation on the 40 and 50% cold-worked specimens was not as evident as that on the other specimens. The number of dimples on the fracture surface of these specimens was also much lower.

3.4 Effect of a Hole

The effect of a hole on the tensile and fatigue properties of as-received specimens was determined on specimens with 3 mm drilled holes and 3 mm punched holes. The drilled hole was an open hole, while the punched hole had an embedded rivet in it; however, as noted earlier, neither the rivet nor the backup strip participated in load sharing. The ratio of the hole diameter to the specimen width was 0.25 for the drilled hole and 0.333 for the punched hole. Knoop microhardness measurements close to the hole edges at 0° (normal to the specimen axis) and 90° directions indicated a considerable amount of cold work in the vicinity of the punched hole (Fig. 13). The microhardness values were between 60 and 65 at 0.5 mm from the hole edge of the drilled hole, and between 85 and 90 at 0.5 mm from the hole edge of the punched hole. From the microhardness measurements, it was estimated that a 4 mm wide region surrounding the punched hole was cold-worked to between a 30 and 40% cold work level based on the comparison with the microhardness data of cold-rolled sheets.

Figure 14 shows the tensile stress-strain curves of these specimens. Both types of specimens failed by crack initiation at the hole boundary in the plane normal to the tensile axis; however, there was a considerable amount of plastic deformation, which was also evident on the stress-strain diagrams. The maximum stress for specimens with a hole, based on the gross area, was much lower than the UTS of the as-received specimen without any hole (Table 3). However, based on the net area, the YS and UTS of both types of specimens were higher than those of the as-received specimen without any hole. The specimens with punched holes produced the highest strengths, but the lowest strain to failure. The presence of a hole at the center of the width creates stress concentration; however, the effect of stress concentration on YS and UTS was reduced due to plastic deformation at the hole edges. The presence of a hole reduced the uniform elongation, and cold work in the vicinity of the punched hole caused further reduction in uniform elongation.

Figure 15 shows the *S-N* diagrams of the specimens with

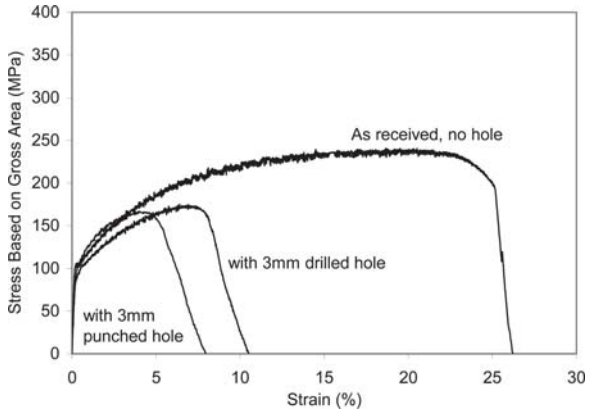

Fig. 13 Effect of hole drilling and hole punching on tensile stress-strain curves (stress based on gross area)

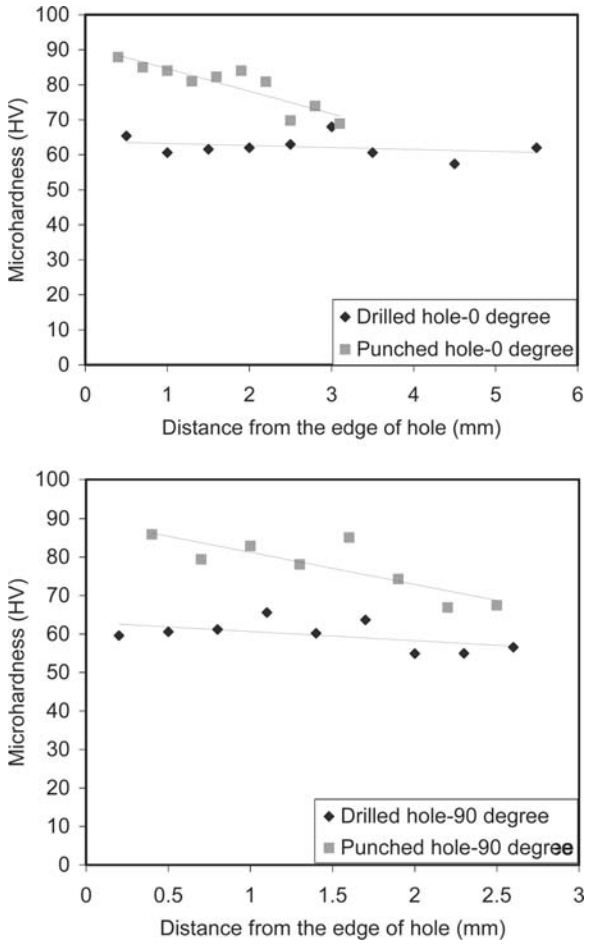

Fig. 14 Knoop microhardness distribution around the drilled hole and punched hole in 5754 sheet

Table 3 Tensile data of as-received, hole-drilled, and rivet-punched 5754 sheet

	0.2% offset YS			UTS			
Condition	Load, N	Based on gross area, MPa	Based on net area, MPa	Load, N	Based on gross area, MPa	Based on net area, MPa	Uniform elongation, %
As-received	2755	110	110	6061	242	242	20.8
With 3 mm drilled hole	2304	92	123	4310	175	233	6.4
With 3 mm punched hole	2004	97	146	3177	166	249	3.9

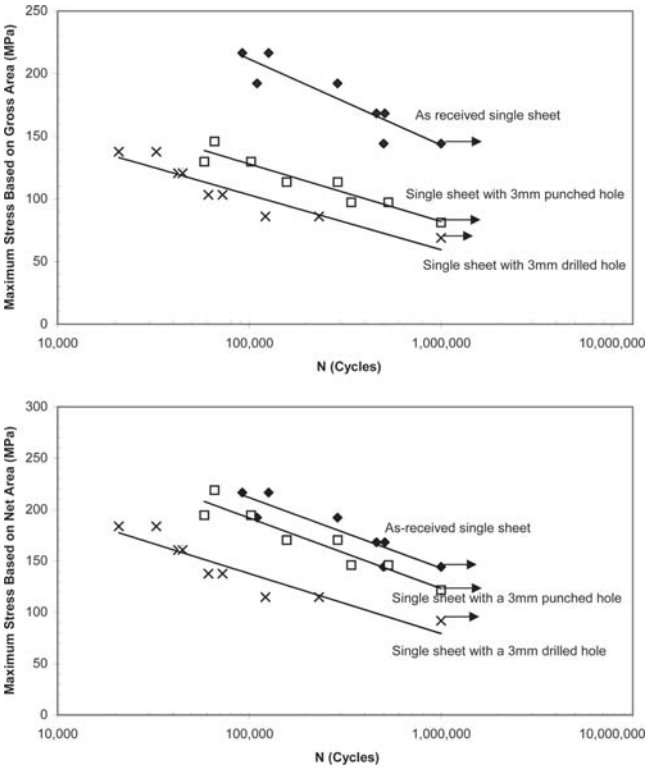

Fig. 15 *S-N* diagrams of as-received, hole-drilled, and rivet-punched AA5754 sheets

drilled holes and punched holes, and compares them with the *S-N* diagram of the as-received specimens without any hole. The fatigue performance of specimens with both drilled holes and punched holes was much lower than that of the as-received specimens. However, the specimens with punched holes had a better fatigue performance than those with the drilled holes on the basis of both gross stress as well as net stress. This can be due to the cold work at the hole edge and its vicinity induced by hole punching

4. Conclusions

In this article, the effect of cold work on the tensile and fatigue properties of the AA5754 alloy was studied. The cold work was induced by cold rolling the as-received AA5754-O sheet up to a 50% thickness reduction. As expected, YS and UTS increased with cold work, and uniform elongation decreased with cold work. The important conclusions from this research relate to critical strain and fatigue strength. Critical strain, which is an indicator of the onset of serrated flow in such material, increased with cold work and decreased with annealing. Cold work increased the fatigue strength of the AA5754 alloy. Fatigue strength decreased slightly by annealing. Hole drilling and hole punching greatly decreased the fatigue strength; however, the fatigue strength of the specimens with punched holes was higher than that of the specimens with drilled holes, presumably due to the cold work induced by punching at the hole edge.

Acknowledgment

The authors would like to acknowledge the research grant provided by Ford Motor Co. under its University Research Programs to conduct this research.

References

1. M.T. Yu, D.L. DuQuesnay, and T.H. Topper, Fatigue Behavior of a Cold-Rolled SAE Grade 945X HSLA Steel, *J. Testing Eval.,* 1990, **18,** p 274-280
2. A.M. Sherman, Fatigue Properties of High Strength-Low Alloy Steels, *Metall. Trans. A,* 1975, **6,** p 1035-1040
3. S.G.S. Raman and K.A. Padmanabhan, Effect of Prior Cold Work on the Room-Temperature Low-Cycle Fatigue Behavior of AISI 304LN Stainless Steel, *Int. J. Fatigue,* 1996, **18,** p 71-79
4. A.M. Sherman and R.G. Davies, Fatigue of Dual-Phase Steel, *Metall. Trans. A,* 1979, **10,** p 929-933
5. Y. Nagase and S. Suzuki, On the Decrease of Fatigue Limit Due to Small Prestrain, *J. Eng. Mater. Technol.,* 1992, **114,** p 317-322
6. V.M. Radhakrishnan and P.S. Baburamani, Initiation and Propagation of Fatigue Crack in Pre-Strained Material, *Int. J. Fract.,* 1976, **12,** p 369-380
7. C.M. Sonsino, The Effect of Coldforming on the Low Cycle Fatigue Behavior of the Fine-Grained Structural Steel Fe E 47 and the Age-Hardened Aluminum Alloy AlCuMg2, *Int. J. Fatigue,* 1984, **6,** p 173-183
8. D.B. Lanning, T. Nicholas, and G.K. Haritos, Effect of Plastic Prestrain on High Cycle Fatigue of Ti-6Al-4V, *Mech. Mater.,* 2002, **34,** p 127-134
9. "Standard Test Methods for Atomic Emission Spectrometric Analysis of Aluminum Alloys by the Point to Plane Technique in Nitrogen Atmosphere," E607, *Annual Book of ASTM Standards,* ASTM, 2002
10. G.T. Bretz, A.M. Sherman, and W.S. Stewart, "Response of Aluminum Alloys to Temperature Exposures Observed in Automotive Service," SAE Paper 950992, Society of Automotive Engineers, 1995
11. S.A. Court, K.M. Gatenby, and D.J. Lloyd, Factors Affecting the Strength and Formability of Alloys Based on Al-3Wt% Mg, *Mater. Sci. Eng.,* 2001, **A319-321**, p 443-447
12. D.J. Lloyd, The Deformation of Commercial Aluminum-Magnesium Alloys, *Metall. Trans. A,* 1980, **11A,** p 127-134
13. J.M. Robinson and M.P. Shaw, Microstructural and Mechanical Influences on Dynamic Strain Aging Phenomena, *Int. Mater. Rev.,* 1994, **39,** p 113-122
14. R.H. Van Stone, T.B. Cox, J.R. Low Jr., and J.A. Psioda, Microstructural Aspect of Fracture by Dimpled Rupture, *Int. Metals Rev.,* 1985, **30,** p 157-179